

# Extraction and Visualization of Swirl and Tumble Motion from Engine Simulation Data

Christoph Garth\*  
University of Kaiserslautern

Robert S. Laramee†  
VRVis Research Center, Vienna, Austria

Xavier Tricoche‡  
SCI Institute, University of Utah

Jürgen Schneider§  
AVL, Graz, Austria

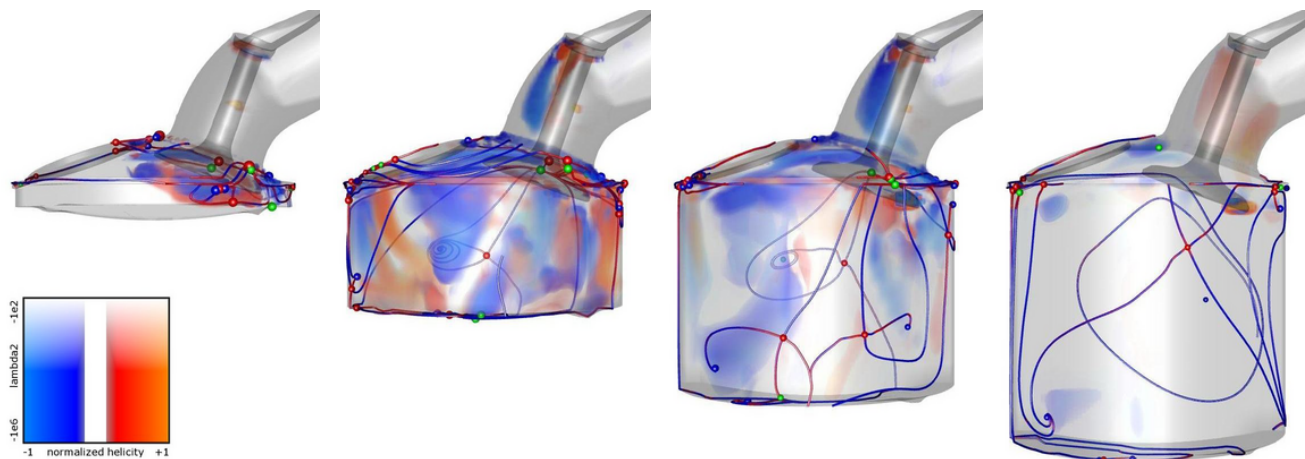


Figure 1: Unsteady visualization of vortices from in-cylinder tumble motion in a gas engine and its relationship to the boundary. During the valve cycle (left to right), the piston head that shapes the bottom of the geometry moves down (not shown). The volume rendering shows vortices using a two-dimensional transfer function of  $\lambda_2$  and normalized helicity (legend). The main tumble vortex is extracted and visible as off-center and with an undesired diagonal orientation. The flow structure on the boundary is visualized using boundary topology. A direct correspondence between the volume and boundary visualizations can be observed. In the third image, the intersection of the main vortex with the boundary results in critical points on the front and back walls.

## ABSTRACT

Optimizing the combustion process within an engine block is central to the performance of many motorized vehicles. Associated with this process are two important patterns of flow: swirl and tumble motion, which optimize the mixing of fluid within each of an engine's cylinders. Good visualizations are necessary to analyze the simulation data of these in-cylinder flows. We present a range of methods including integral, feature-based, and image-based schemes with the goal of extracting and visualizing these two important patterns of motion. We place a strong emphasis on automatic and semi-automatic methods that require little or no user input.

The simulation data associated with in-cylinder tumble motion within a gas engine, given on an unstructured, time-varying and adaptive resolution CFD grid, demands robust visualization methods that apply to unsteady flow. We make effective use of animation to visualize the time-dependent simulation data. We also describe the challenges and implementation measures necessary in order to apply the presented methods to time-varying, volumetric grids.

**CR Categories:** I.4.7 [Image Processing and Computer Vision]:

\*e-mail: garth@informatik.uni-kl.de

†e-mail: laramee@vrvis.at

‡e-mail: tricoche@sci.utah.edu

§email: juergen.schneider@avl.com

Feature Measurement—; I.6.6 [Simulation And Modeling]: Simulation Output Analysis—; J.2 [Physical Sciences and Engineering]: Engineering—.

**Keywords:** time-varying grids, time-dependent data, flow visualization, feature extraction, feature-based visualization, in-cylinder flow, engine simulation, flow topology

## 1 INTRODUCTION

Among the many design goals of combustion engines, the mixing process of fuel and oxygen occupies an important place. If a good mixture can be achieved, the resulting combustion is both clean and efficient, with all the fuel burned and minimal exhaust remaining. In turn, the mixing process strongly depends on the inflow of the fuel and air components into the combustion chamber or cylinder. If the inlet flow generates sufficient kinetic energy during this valve cycle, the resulting turbulence distributes fuel and air optimally in the combustion chamber. For common types of engines, near-optimal flow patterns are actually known and include, among others, so-called swirl and tumble motions. With the general progress of state-of-the-art CFD simulations, the discipline of engine design is made accessible to both numerical simulation and visualization of the resulting datasets, allowing for rapid testing of engine designs.

Laramee et al. [8] took preliminary steps towards the visualization and analysis of in-cylinder flow. Using a combination of texture-based and geometric techniques, they were able to indirectly visualize the key swirl and tumble patterns in two engine simulation datasets. The approaches they used were essential man-

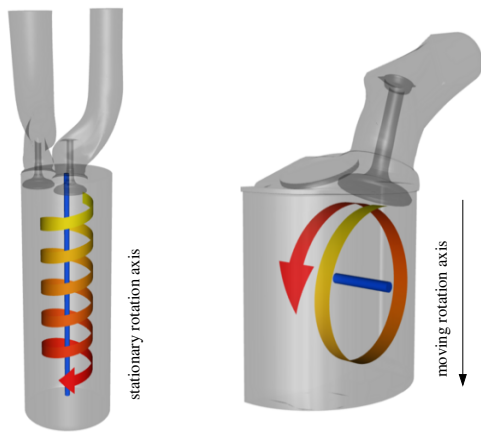


Figure 2: (Left) Stable, circulating flow pattern in a diesel engine designated as *swirl motion*, with the cylinder axis as the axis of rotation. The flow enters tangentially through the intake ports. (Right) Transient *tumble motion* in a gas engine. The axis of motion moves as the cylinder expands (cf. Fig. 1) and stays halfway between the top cylinder wall and the piston head at the bottom (not shown).

ual, and they did not consider time-dependent flow. It is the aim of this paper to expand on this previous study by providing additional feature-centric visualizations of the swirl and tumble motion patterns that extract swirl and tumble characteristics (semi-) automatically. With application by engineers in mind, we present a survey of methods that are useful in this context and demonstrate how they can be effectively applied in engine simulation analysis.

Of particular interest are the time-varying nature of the simulation and the interconnection between visualization methods that treat data of different dimensionality (typically boundary vs. volume data). We study to what extent an analysis of the boundary flow permits reliable insights into the volume of the combustion chamber on the presented examples.

We describe the techniques employed and present a critical discussion of the resulting visualizations from an application standpoint. Although the application domain covered in this work is specific, the conclusions reached can be leveraged in many areas of engineering.

The paper is structured as follows. In Section 2, we describe the datasets that we based our analysis on, namely two important patterns of in-cylinder flow. Section 3 is concerned with the criteria for our choice of methods. We briefly describe the methods and how they contribute to a satisfactory extraction and visualization of swirl- and tumble-motions. Some of the technical aspects involved in time-varying unstructured grids are detailed as well. Hybrid combinations of methods are examined in Section 5, before we conclude on the presented work in Section 6.

## 2 ENGINE SIMULATION DATA

From a simplified point-of-view, there are two types of ideal flow patterns in an engine cylinder: swirl motion and tumble motion. Both are rotational motions, however, the axis of rotation is different in each case. Depending on the type of engine, one of these patterns is considered optimal because it maximizes mixing of injected fuel and air, resulting in homogeneous combustion.

In this paper, we treat two datasets showing each of these two types of flow patterns (henceforth termed “swirl-motion dataset and “tumble motion dataset”). The basic geometries of the datasets and the respective desired motion patterns are shown in Figure 2. Although they were generated in the same problem context, the simu-

lation datasets differ in a number of ways.

### 2.1 Swirl-Motion in a Diesel Engine

This simulation is the result of a the simulation of steady charge flow in a diesel engine, based on a stationary geometry, resulting in a simple and stable flow. The main axis of motion is aligned with the cylinder axis and is constant in time. The spatial resolution of the single timestep is high with a total of 776.000 unstructured cells on an adaptive resolution grid.

### 2.2 Tumble-Motion in a Gas Engine

This dataset results from an unsteady simulation of the charge phase of a gas engine (crank angles  $380^\circ$  to  $540^\circ$ ). As the piston moves down, the cylinder volume increases by an order of magnitude and the fuel-air mixture entering the cylinder is drawn into a gradually developing tumble pattern. The overall motion is highly transient and unstable. Both spatial and temporal resolution are relatively low, with the data given on 32 timesteps and the grid consisting of roughly 61.000 unstructured elements at the maximum crank angle. It is interesting to note that the actual mesh topology remains constant throughout all timesteps. This is accomplished by the use of virtual zero-volume cells at the piston head that expand as the piston moves down; only the mesh vertices are changing in time.

Both simulations were computed in the Department of Advanced Simulation Technologies (AST) at AVL ([www.avl.com](http://www.avl.com)) for the design and analysis of specific flow in-cylinder types. In addition to the flow vector field, the datasets encompass a number of additional attributes such as temperature and pressure. In this work, we focus on the analysis of the swirl and tumble aspects of the flow vector field. Although the highest priority is given to the visualization of the patterns themselves (or their absence), causes for their absence are also sought.

## 3 CHOICE OF METHODS

Here, we describe the criteria for our selection of visualization methods.

### 3.1 Visualization Goals

The main interest in the visualization of the datasets is the extraction and visual analysis of the swirl- and tumble-motion patterns. Therefore, the flow vector field and its derived quantities are of primary interest.

For the use in design analysis, the constructed visualizations need to be objective, meaning that the quality of the visualization result must not depend on vital parameters to be supplied by the user. This results in comparable visualizations for different simulation results of the same prototype or possibly even among different design prototypes. Therefore, in the selection of methods, we have put an emphasis on automatic schemes that require little or no user input.

### 3.2 Data Dimensionality

The simulation results are given in the form of attributes defined in the interior of the respective cylinder geometries. As is quite common in CFD simulations, the flow is required to vanish on the domain boundary (no-slip condition) in order to correctly model fluid-boundary friction. Nevertheless, values on the boundary of the domain are easily inferred by e.g. extrapolation of volume values next to the boundary. It is also notable that in classical engineering analysis, visualization is widely performed on two-dimensional slices.

Overall, the level of information that can be provided by a visualization technique increases with the dimension of the data it treats. At the same time, the visualization result need not necessarily improve due to perceptual issues such as cluttering. Finally, there is usually a price to pay in algorithmic complexity and computational cost as one progresses to higher dimensions. Therefore, for the case of our examples, we examine in some detail how the analysis of boundary and slice data allows to draw reliable conclusions on the pattern of the volume flow. We achieve this by a pairing of methods that combine boundary and volume techniques.

### 3.3 Practical considerations

In our study of the datasets, we have found that the possibility of interactive viewing of visualization results greatly enhances the comprehension of occurring structures. This is in part to be attributed to the complex geometries of the datasets that are conducive to spatial perception problems. In the case of time-dependent tumble motion, it is especially helpful to see the dataset and the visualization in an animation. Only through this can the dynamic of the different motions be fully understood. Even most of the techniques that apply only to stationary flow (such as the better part of feature-extraction schemes) lend themselves favorably to the generation of animations by concatenation of results on successive time-slices. The reader is referred to the accompanying video [1] in which we demonstrate this. As a consequence, we construct the visualizations off-line in a preprocessing step and then display the results in an interactive viewer.

While we employ GPU-based programming techniques [23] to promote a good viewing experience, we have taken care not to rely on the latest generation of GPUs or otherwise platform-dependent hardware. The visualization pipeline including preprocessing and interactive viewing runs well on a moderately equipped workstation. The examples in this paper were treated on a PC with 2 gigabytes of RAM and an NV20 class GPU.

## 4 EXTRACTION AND VISUALIZATION OF SWIRL AND TUMBLE MOTION

In this section we present the methods along with corresponding visualization results and discuss their relevance with respect to the realization of the visualization goals.

*Remark:* Due to limitation of available space for images, many of the figures used for illustration of individual methods actually show a combination of different visualization approaches. We discuss the benefits of such combinations in detail in Section 5.

### 4.1 Visualization of Global Flow Behavior with Integration-based Methods

Integration-based methods are well suited to the analysis of time-dependent flows. Their common application to stationary flows is only a special case. We go on to discuss specific approaches in the next section.

#### 4.1.1 Particles & Pathlets

Despite their simplistic nature, particle visualization can provide valuable insight into the overall structure of a flow dataset (cf. e.g. [2, 12]). This is especially true for time-dependent data. While the basic principle is similar to that of streamlines or pathlines, an animation of moving massless particles manages to convey the dynamic nature of the flow much better than static imagery alone. In the general case, integral methods suffer from seeding issues, although strategies have been proposed to circumvent this (e.g. [22]). However, none of these approaches is concerned with time-varying

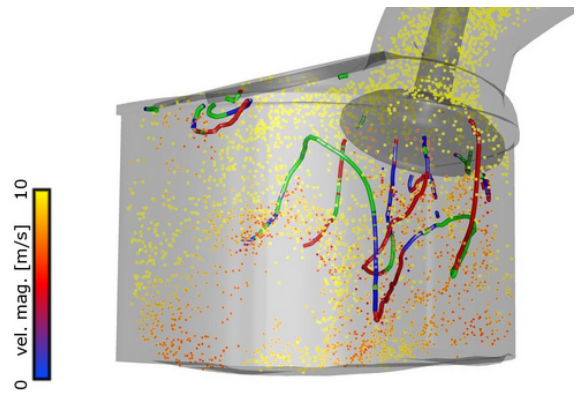


Figure 3: A single frame from a time-varying tumble motion visualization using a combination of particles and vortex cores as extracted using cutting-plane topology. Particle velocity magnitude is color-coded. The green lines represent the extracted vortex cores. Over time, some of the particles are captured in the vicinity of vortex cores resulting in lost energy (lower velocity) for the creation of the tumble pattern.

data. Fortunately, engine geometries offer the inlet pipe as a natural choice of a seeding region. Integration of pathlines in time-dependent 3D flows is straightforward through the application of standard numerical integration algorithms that only require the integrand at a sparse set of points. While interpolation in time-varying grids is usually problematic, we were able to exploit the topologically invariant structure of the grid to simplify point location.

Figure 3 depicts a single frame from an animation of massless particles moving with the flow during the early stage of the valve cycle, seeded at positions in the intake pipe. The particles are of uniform size and color-coded according to the flow velocity. The image allows an easy identification of zones where the velocity is lower than average, hinting at a non-optimal inflow pattern at the side of the valve. A sequence of pathlet images corresponding to different timesteps (Fig. 4) shows the evolving flow pattern. Individual pathlets are color coded by the angle of their velocity in the plane of the tumble motion. An optimal motion pattern, when viewed orthogonally, should resemble the color wheel given in the legend. Through this simple approach, it is possible to visually match the pattern and confirm its presence or absence in different parts of the dataset. The rightmost image confirms that the overall motion is evolving towards roughly tumble-like nature. However, the region below the intake valve shows a very low velocity (short pathlets), and at the front of the cylinder the flow has a swirl-like component (cyan pathlets). The flow exhibits non-ideal asymmetry.

Our general experience with this technique is that in spite of being imprecise, it greatly furthers the comprehension of the time-dependent flow by providing an overview.

#### 4.1.2 Streamsurfaces

Streamsurfaces as an extension of streamlines are of great value in some applications because they manage to convey a spatially coherent picture of flow structures (cf. [4, 16, 3]). We found them to be of limited use in our case, for two reasons. First, both swirl and tumble are large-scale motions that are locally overlaid by other small-scale flow patterns and the resulting streamsurfaces are complicated to interpret since the small details are emphasized by the surface nature of this primitive. Secondly, it is unclear how they can be applied satisfactorily in a time-dependent context.

Despite these drawbacks, we were able to apply a streamsurface to study the intake behavior in the swirl-motion dataset (see

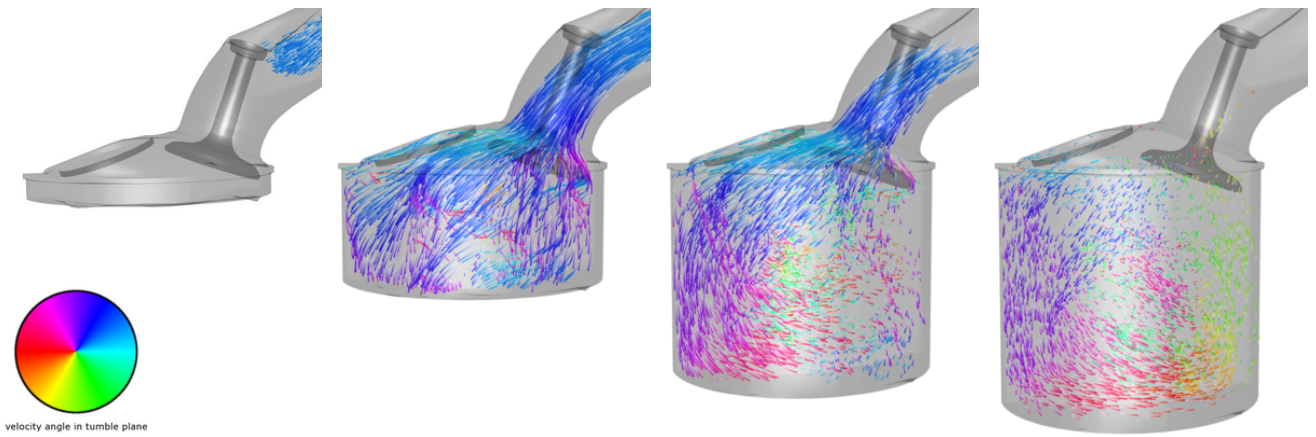


Figure 4: Time-varying pathlet visualization of the tumble flow pattern (left to right). Velocity magnitude is visualized by pathlet length. Pathlets are seeded in the upper intake pipe. As the piston moves down, the tumble pattern emerges. The angle of the pathlet velocity in the tumble plane is coded by color and allows an identification of a coherent tumble motion (last image). The ideal tumble motion is not achieved due to low velocities on the right cylinder side and a swirl-like behavior of some pathlets (cyan pathlets in the front).

Fig. 5). The streamsurface is seeded at the beginning of the intake pipe and a part of it caught in a vortex after passing beyond the valve. This vortex is considered sub-optimal due to a loss in kinetic energy which may otherwise contribute to swirl.

## 4.2 Topology-Based Visualization of Flow Structures

Topological methods provide efficient means for the visualization of essential structures in steady flows. As opposed to the integral methods described previously, they offer a fully automatic way to gain insight from vector data sets. The topological technique is typically applied in the visualization of planar flows [15] for which it yields synthetic graph representations. It consists of critical points (vector field zeros) and connecting separatrixes. The three-dimensional case, however, remains challenging. Besides frequent occlusion problems that must be addressed specifically [19], prominent features of interest like vortices cannot generally be identified as elements of 3D topology.

In this paper, we address these deficiencies by combining a topological analysis of the boundary flow with a hybrid approach that leverages 2D topology to explore the 3D structure of a vector field [20].

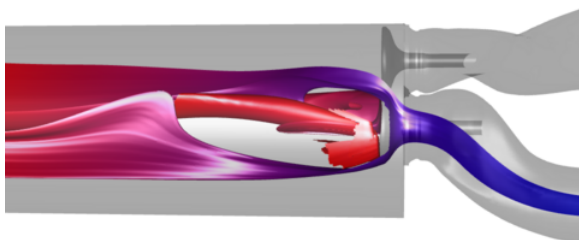


Figure 5: A streamsurface seeded in the intake pipe shows non-optimal intake flow around the valve. The streamsurface is color coded according to arc length in integration direction for better visual perception. A part of the streamsurface is drawn back to the top of the cylinder, attaches to the valve, and circulates in a vortex.

### 4.2.1 Boundary Topology

To our knowledge, a general algorithm for vector field topology on arbitrary triangulated 2-manifolds in three-space has not yet been described in the visualization literature. Thus, we propose the following approach. In each triangle, we use the well-defined local tangent plane to perform a cell-wise search for critical points and determine their type. The construction of separatrixes from saddle points is performed using a streamline integration approach based on geodesics as introduced by Polthier and Schmieß [11]. A specific characteristic of triangulated surfaces for topological analysis is the existence of what we term *singular edges*. Since the tangent plane is discontinuous across surface edges, the flow on both sides can be contradictory. Singular edges are typically found along the sharp contours of the geometry where they must be integrated in the topological analysis to account for the possibly contradictory flow behavior between neighboring cells.

For viscous flows, the information conveyed by the boundary topology can be naturally enhanced by showing the strength of flow separation and attachment along separatrixes. Flow separation occurs when the flow surrounding an embedded body interrupts its tangential motion along the object's boundary and abruptly moves away from it. The opposite phenomenon is called flow attachment. As pointed out by Kenwright [6], separatrixes of the boundary vector field constitute so called closed separation or attachment lines. To quantify flow separation and attachment along a separatrix, we compute the divergent (resp. convergent) behavior of neighboring streamlines by evaluating the local divergence of the vector field [21]. This is illustrated in Fig. 11 by the color coding of the intensity of flow separation and attachment along separatrixes.

Direct visualization of the boundary topology produces images such as Figure 6 (swirl dataset) and can also be applied in a time-dependent context. The combination of linear interpolation in time and in space often produces artifacts (such as artificial pairs of critical points that appear and quickly vanish quickly). Nevertheless, animations that show the temporal evolution of these instantaneous graphs provide valuable means to track the dynamic of important flow patterns (cf. Fig. 11). In our experience, boundary topology is most effective if used in conjunction with methods that visualize additional properties of the flow, both in the volume and on the boundary. Such combinations permit to determine the mutual influence between boundary and volume. We will discuss these issues when we examine further combinations of methods presented in Section 5.

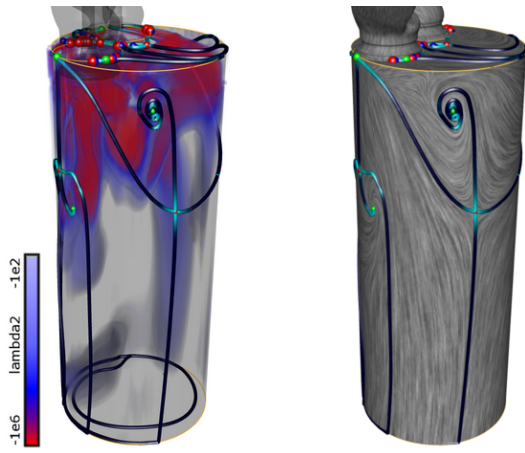


Figure 6: Visualization of swirl motion using boundary topology. Critical points are colored by type, and separatrix color varies with separation/attachment behavior from dark blue (weak) to cyan (strong). Singular edges Separatrices indicate the separation between neighboring vortices on the boundary. (Left) Combination with volume rendering with a transfer function of  $\lambda_2$  only. On the bottom left of the cylinder, the recirculation zone causes a non-ideal off-center rotation, as visualized by topology. (Right) In combination with LIC.

#### 4.2.2 Cutting-Plane Topology

It was shown previously [20] that a moving cutting plane that traversing the dataset and on which the vector field is resampled and projected at regular intervals can be a powerful tool in the analysis of 3D datasets. The projection of the vector field on the plane effectively manages to discard structures orthogonal to the plane, but preserves plane-parallel flow patterns. If assumptions on the orientation of features are given, this property can be exploited. Cutting-planes are hence ideally suited for the qualitative analysis of swirl or tumble motion, since its axis of rotation is known. Furthermore, the (discretized) continuum of cutting-planes allows for the application of critical-point tracking over the plane parameter range. In the case of vortical motion that is intersected orthogonal to the rotational center, a reproduction of the vortex core as the path of a critical point over the parameter range should, in theory, work well. In practice, it is hard to intersect (a-priori unknown) structures exactly. This results in approximations of the vortex cores. Still, a qualitative analysis is viable.

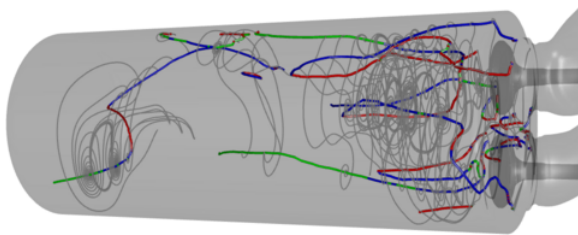


Figure 7: Cutting-plane topology applied to the diesel engine. Separatrices on different planes are colored gray. Although the visualization must be interpreted with caution, swirl structures emerge clearly. Critical points paths are colored according to type. Observe that the overall swirl motion is fueled by several parallel vortices at the top of the cylinder. The main swirl motion core is disrupted near the middle.

In Figure 7, the results of this approach applied to the swirl motion dataset are displayed. As the cutting planes are applied orthogonal to the cylinder axis, coherent swirl-type structures emerge at the top of the cylinder. Rotation cores orthogonal to the planes are visualized by critical point paths over the plane continuum. Interestingly, the main swirl core is supposed to extend through the whole cylinder, but is actually interrupted near the middle.

Figure 9 shows several frames from an animation of the tumble dataset. The moving cutting planes have been applied orthogonal to the tumble axis and are color coded by their distance to the back wall of the combustion chamber for increased visual clarity. Although the visualization is not exact, the prevalent tumble structure is captured well in spite of its overall weakness and instability. Again, the center of the respective motions is given by the critical points paths. The tumble motion is found to consist of several smaller vortices, of which some have a diagonal orientation that looks like a simultaneous combination of swirl and tumble. In the full animation, the interaction of the different smaller tumble patterns can be observed as they split and merge.

Using only the critical point paths in visualization, it is possible to observe the main tumble vortex, as shown in Figure 12. It does not completely match the desired axis and is highly off-center on the curved wall of the combustion chamber. Here too, the diagonal nature of the main rotation is confirmed.

#### 4.3 Direct Extraction and Visualization of Vortices

The extraction and visualization of vortices is one of the classical topics of flow visualization, and much work has been published on the topic. A good overview is presented by Post et al. [13]. In general, methods can be divided into those that focus on the extraction of line-type primitives signifying a vortex core line (see also [14]), and those that extract vortex cores as regions based on different criteria. While the former produce precise results, the resulting line primitives are difficult to interpret in complicated datasets, since they offer only little information about the extent of a vortex or the interaction of multiple vortices. In time-dependent, vortex dominated flows this is a limiting factor (and tumble motion is a prime example here). Therefore, vortex core region methods are useful to visualize regions of influence and vortex interactions.

##### 4.3.1 The Parallel Operator and the Sujudi-Haimes method

We apply the algorithm of Sujudi and Haimes [18] in the numerically more stable parallel operator version [10]. The basic idea consists of a local (per-cell) pattern matching based on the definition of a vortex core as the center of rotational motion. The algorithm results in a number of unconnected line segments. Post-processing must be applied in order to sort out false positives and achieve coherent vortex core lines (this is detailed by Roth [14]). While the

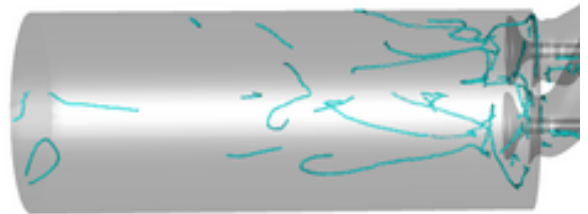


Figure 8: Direct vortex visualization in the swirl dataset using the Sujudi-Haimes algorithm. The method favors small and strong vortices, therefore, it is not ideally suited for the visualization of the large-scale swirl motion. The recirculation zone at the bottom of the cylinder is however captured well.

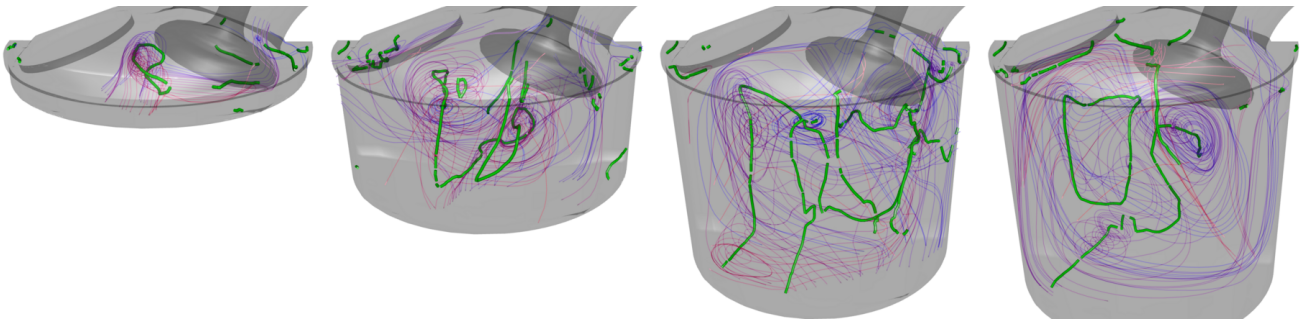


Figure 9: Four frames from an animation of the tumble motion simulation. Cutting plane topology is applied to visualize flow field structures in the plane orthogonal to the tumble axis. Color of separatrices varies from blue to red on successive cutting planes. Tumble-like flow structures emerge clearly from the otherwise incoherent lines. The paths of critical points over the cutting plane continuum are displayed in green. In the last frame (right), the diagonal main tumble axis can be observed together with a large recirculation zone (closed path on the left).

method produces good results for simple datasets, it requires derivatives of the flow vector field and is therefore prone to the influence of numerical noise. It has, however, the benefit of being completely automatic and generating objective results.

Figure 8 shows an overview of the swirl dataset with the extracted vortex cores. From this image, it is visible that the overall swirl motion consists of several smaller-scale vortices in the upper half of the cylinder. In the middle and close to the bottom, small-scale disturbances are visible. An interpretation of a dataset by this visualization can be insightful but also insufficient by itself. If for example, the small vortices at the top are actually counter-rotating, an optimal swirl pattern is not achieved (see also below). However, this cannot be judged with confidence from these images alone.

#### 4.3.2 Volume Visualization

Among the many region-based vortex definitions, the  $\lambda_2$ -criterion [5] has a well established tradition in engineering use. The criterion is given as a scalar quantity derived from the flow field Jacobian matrix and related to a minimum in pressure in Navier-Stokes equation [9]. According to its definition, a vortex is present at a point if  $\lambda_2 < 0$ . Traditionally, isosurfaces are used to visualize vortices. However, this approach does not fare well in complicated datasets with many vortices. The resulting isosurfaces do not separate individual vortices and are prone to visual complexity. This is only avoided by a careful manual selection of the isovalue. In addition, the strength of the rotation (as given by the modulus of  $\lambda_2$ ) is not visualized. Volume rendering has also been applied in this context [17, 20] and is able to overcome most of the difficulties related to isosurfaces. As described in [20], we have not attempted to apply volume rendering directly to the unstructured grid but have employed a resampling scheme that results in a rectilinear grid covering the region of interest (in our cases, the cylinder). It is then used in a direct volume rendering approach. Although artifacts are incurred in naive sampling, post-sampling scale-space filtering is very effective in removing these artifacts.

Using this approach, Figure 6 (left) illustrates the vortices in the context of the swirl motion using a simple one-dimensional transfer function that indicates vortex strength by color. As already visible in the results of the Sujudi-Haimes method, the actual swirl motion consists of several independent vortices, most prominently a strong vortex that spans almost the entire length of the cylinder. It is clearly off-center. A close-up of the upper cylinder region including the region just below the intake port is detailed in Figure 10. It is apparent that the fuel-air mixture entering the cylinder is drawn into a strong rotational motion. Whether this is good for the overall mixing process or an obstacle that results in a pressure loss with negative consequences remains unclear. Technically, we

have limited the transfer function range to  $\lambda_2$ -values between  $-10^6$  and  $-10^2$  to filter vortical motions at the small scales.

Recently, the use of multi-dimensional transfer functions [7] in flow visualization was investigated [20]. We make use of this technique to visualize the rotational orientation of individual vortices, allowing more insight into the mutual interaction in the observed vortex systems. Adding *normalized helicity* as a second variable, we manage to both strengthen the vortex region criterion as well determine the orientation of the rotational motion. Normalized helicity is given as the angle between the velocity vector and the vorticity vector and has a range of  $[-1, 1]$ , with positive values in the case of counter-clockwise rotation in flow direction and near-zero values indicating very weak vortical behavior. The obtained visualization (cf. Fig 10) indicates several mutually counter-rotating vortices in close proximity near the intake ports. This is highly undesired, since part of the energy contained in the inflow is used up by this vortex system.

The use of multidimensional transfer functions (most commonly in medical image generation) can require some degree of interactiv-

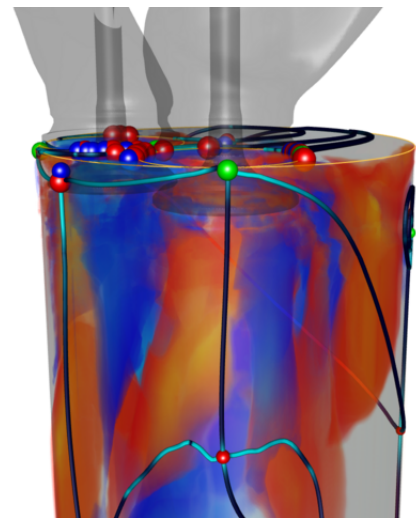


Figure 10: Visualization of the rotational directions in the vortex system at the top of the diesel engine cylinder. The transfer function is identical to that of Fig. 1. The counter-rotating vortices appear in blue and in red depending on rotation direction. On the boundary, the topological analysis extracts and visualizes separation lines between individual vortices.

ity in the determination of the transfer functions in order to specify variable ranges manually for most satisfactory results. We wish to emphasize that in our case, transfer functions based on physical criteria (such as  $\lambda_2 < 0$ ) are automatic in the sense the interesting value ranges are dictated by the laws of fluid dynamics. Using simple linear interpolation in time, an animation can depict the temporal evolution of vortices associated with swirl and tumble motion (see Fig. 1).

## 5 HYBRID APPROACHES

While performing experiments with the different approaches detailed above, it became apparent that a combination of visualizations can provide an even more thorough understanding of the simulation results. In this section, we describe examples of particularly effective combinations and how they contribute to the swirl and tumble analysis.

### 5.1 Boundary and cutting plane topology

In fluid flows, complex flow structures such as vortices are often caused by the interaction of the flow with boundaries. Depending on this interaction, different patterns appear on a boundary that in turn allow to infer properties of the volume flow. However, in complicated geometries such as in-cylinder flow, this approach alone introduces visualization complexity due to the high number of vortices involved and generally complex flow structure.

The combination of boundary topology and cutting plane topology is an effective approach. Figure 11 illustrates this in time-slices from an animation. For the tumble flow, this type of visualization provides valuable insight into the development of the diagonal tumble motion. In the early stages of the valve cycle (left two images), the flow pattern is very incoherent and unstable. Roughly at the middle of the cycle (second image from the right), a swirl pattern occurs in the front half of the cylinder, mainly constituted by two large vortices. In the very last timesteps, the rotational axis tilts towards the desired tumble axis, but fails to reach it completely. Here, a large recirculation zone can be observed that may hinder the development of the tumble motion.

### 5.2 Sparse and dense methods

On the boundary, the topological graph as a visually sparse method is effectively combined with dense methods, such as texture-based methods or volume visualization. While texture-based methods are built on the capability of the human visual system to identify patterns in the flow, the topological graph serves as a terse structural picture that relies on cognitive interpolation on behalf of the viewer. It is therefore a very natural combination. Figure 6 (swirl, right image) provides an example, showing a very strong vortex near the inlet that is drawing away energy from the creation of the ideal swirl pattern. We refer the reader to previous work [8] for other applications of texture-based techniques in this problem context that we believe will benefit strongly from a pairing with a feature-based visualization.

A similar conclusion is reached by combining boundary topology and the volume visualization of vortices. Again looking for the swirl pattern, the imperfection of the actual flow motion is visible in Figure 6 (left). While the volume rendering shows the correctly oriented but off-center main vortex, the topology graph on the lower cylinder boundary complements this visualization by showing corner regions of the flow that are not taking part in the swirl pattern. As expected, the topological graph also serves to show separation and attachment boundaries that delimit the regions of influence of the different vortices. As confirmed by the rotational direction anal-

ysis (cf. Fig. 10), these vortices are rotating in different directions, which is considered as destructive flow behavior.

There are of course other possible combinations: for example, the Sujudi-Haimes vortex core line visualization can play a similar role as cutting-plane topology. In our experiments we found however that it often detects only the strong vortices at the intake portions of both datasets. Combining particles and vortex core lines offers insights into how exactly the vortices are created and where kinetic energy is lost in small scale structures (cf. Fig. 3).

## 6 CONCLUSION AND FUTURE WORK

By using a number of visualization techniques that we selected as automatic and objective, we were able to extract and create visualizations of the swirl and tumble datasets that allow an in-depth visual analysis of the actually occurring patterns. The visualizations are comparable between similar datasets and can thus be employed in design prototype analysis. By using hybrid combinations of different techniques, we were able to determine the extent to which the desired pattern is established and also detect influences that hinder its formation. In summary:

- The swirl motion in the diesel engine is visible in the form a prominent main vortex spanning the entire cylinder (Figure 6, left). It is non-optimally off-center. A recirculation zone is present in the lower corner of the cylinder. This may be the cause for the excentricity of the swirl motion. A vortex system at the intake valve (Figures 8, 6 and 10 prohibits the full conversion of energy contained in the incoming flow into the swirl motion.
- The observed tumble motion in the gas engine is strongly diagonal and resembles a hybrid of both swirl and tumble (Figures 11 and 12). Here too, a prominent recirculation zone induces the swirl component into the flow. Again, the flow distribution at the intake valve is not optimal.

The unstructured, adaptive and time-varying nature of the tumble datasets poses a technical difficulty that we were able to circumnavigate through the choice of schemes and appropriate extensions where needed. The resulting visualizations are of high quality and provide valuable insight into the application.

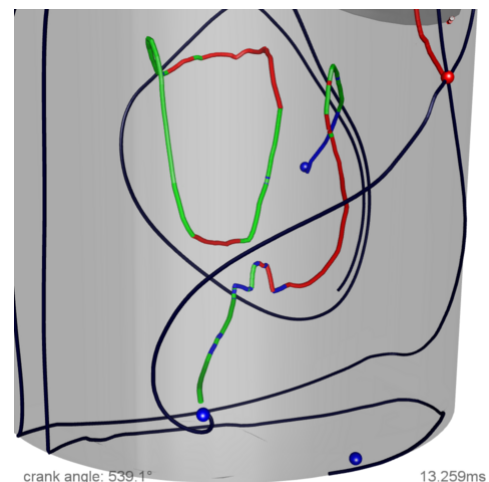


Figure 12: Close-up of Figure 11. Tumble motion center lines are extracted using cutting-plane topology and are colored according to the type of the critical point path. Boundary singularities appear at intersections of the rotation centers with the boundary.

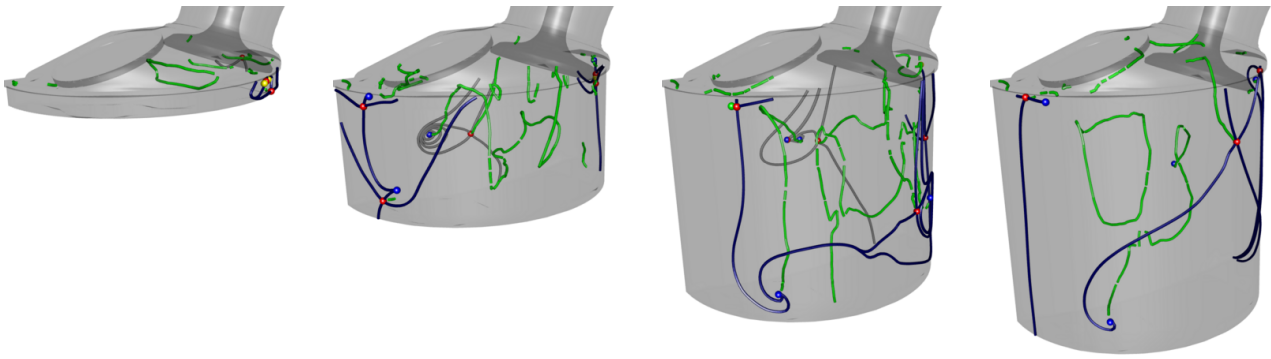


Figure 11: Time-varying visualization of tumble motion using a combination of cutting-plane topology and boundary topology. Where the critical point paths computed over the cutting-plane parameter range intersect the boundary, singularities appear there, too. This is a prime example of a hybrid approach being used to investigate the relationship between boundary and volume methods.

There are many possible avenues that future work might take. High up on the priority list are improvements in the field of topological visualization. Full three-dimensional topology has not been completely realized, and while delivering viable visualization results, replacements such as cutting-plane topology are not completely satisfactory. The inclusion of features such as vortex cores into the topological skeleton is desirable, but may not be possible. Furthermore, the interplay between the topologies of the boundary and volume flows need to be investigated on a more systematic basis. In general, it seems desirable to examine the hybridization of different visualization approaches in the same context.

Future work could also feature improvements to many of the schemes presented here to allow for the treatments of larger datasets, such as whole engine blocks. It remains to be seen in how far this is feasible from a technical point of view.

#### ACKNOWLEDGEMENTS

The authors would like to thank all those who have contributed to this research including AVL ([www.avl.com](http://www.avl.com)), the Austrian research program Kplus ([www.kplus.at](http://www.kplus.at)). The CFD simulation datasets are courtesy of AVL.

#### REFERENCES

- [1] Extraction and Visualization of Swirl and Tumble Motion from Engine Simulation Data (Companion video). available at <http://www.vrvis.at/scivis/laramee/MotionExtracted/>.
- [2] D. Bauer and R. Peikert. Vortex Tracking in Scale-Space. In *Data Visualization 2002. Proc. VisSym '02*, 2002.
- [3] C. Garth, X. Tricoche, T. Salzbrunn, and G. Scheuermann. Surface Techniques for Vortex Visualization. In *Proceedings Eurographics - IEEE TCVG Symposium on Visualization*, 2004.
- [4] J. P. M. Hultquist. Constructing Stream Surfaces in Steady 3D Vector Fields. In A. E. Kaufman and G. M. Nielson, editors, *IEEE Visualization '92*, pages 171 – 178, Boston, MA, 1992.
- [5] Jinhee Jeong and Fazle Hussain. On the Identification of a Vortex. *Journal of Fluid Mechanics*, pages 69–94, 285 1995.
- [6] D. Kenwright, C. Henze, and C. Levit.
- [7] Joe Kniss, Gordon Kindlmann, and Charles Hansen. Multidimensional transfer functions for interactive volume rendering. *IEEE Transactions on Visualization and Computer Graphics*, 8(3):270–285, July–September 2002.
- [8] R. S. Laramée, D. Weiskopf, J. Schneider, and H. Hauser. Investigating Swirl and Tumble Flow with a Comparison of Visualization Techniques. In *Proceedings IEEE Visualization '04*, pages 51–58. IEEE Computer Society, 2004.
- [9] R. Peikert. Tutorial on Feature Oriented Methods in Flow Visualization, IEEE Visualization 2004.
- [10] R. Peikert and M. Roth. The “Parallel Vectors” operator - A vector field visualization primitive. In *IEEE Visualization Proceedings '00*, pages 263 – 270, 2000.
- [11] K. Polthier and M. Schmieß. Straightest Geodesics on Polyhedral Surfaces. In Hans-Christian Hege and Konrad Polthier, editors, *Mathematical Visualization*, pages 135–150. Springer Verlag, Heidelberg, 1998.
- [12] F. H. Post, B. Vrolijk, H. Hauser, R. S. Laramée, and H. Doleisch. Feature Extraction and Visualization of Flow Fields. In *Eurographics 2002 State-of-the-Art Reports*, pages 69–100, 2–6 September 2002.
- [13] F. H. Post, B. Vrolijk, H. Hauser, R. S. Laramée, and H. Doleisch. The State of the Art in Flow Visualization: Feature Extraction and Tracking. *Computer Graphics Forum*, 22(4):775–792, Dec. 2003.
- [14] M. Roth. *Automatic Extraction of Vortex Core Lines and Other Line-Type Features for Scientific Visualization*. PhD thesis, ETH Zürich, 2000.
- [15] G. Scheuermann and X. Tricoche. Topological methods for flow visualization. In C.D. Hansen and C.R. Johnson, editors, *The Visualization Handbook*, pages 341–356. Elsevier, 2005.
- [16] D. Stalling. *Fast Texture-based Algorithms for Vector Field Visualization*. PhD thesis, 1998.
- [17] S. Stegmaier and T. Ertl. A Graphics Hardware-based Vortex Detection and Visualization System. In *Proceedings of IEEE Visualization '04*, pages 195–202, 2004.
- [18] D. Sujudi and R. Haimes. Identification of Swirling Flow in 3D Vector Fields. Technical Report AIAA Paper 95–1715, American Institute of Aeronautics and Astronautics, 1995.
- [19] H. Theisel, T. Weinkauff, H.-C. Hege, and H.-P. Seidel. Saddle Connectors - An Approach to Visualizing the Topological Skeleton of Complex 3D Vector Fields. In *IEEE Visualization '03*, 2003.
- [20] Xavier Tricoche, Christoph Garth, Gordon Kindlmann, Eduard Deines, Geric Scheuermann, Markus Rütten, and Charles Hansen. Visualization of Intricate Flow Structures for Vortex Breakdown Analysis. In *Proceedings of IEEE Visualization*, pages 187–194, October 2004.
- [21] Xavier Tricoche, Christoph Garth, and Geric Scheuermann. Fast and robust extraction of separation line features. In *Proceedings of the Dagstuhl Scientific Visualization Seminar*, 2003. to appear.
- [22] Verma V., D. Kao, and A. Pang. A Flow-guided Streamline Seeding Strategy. In *Proceedings of IEEE Visualization '00*, 2000.
- [23] R. Westermann and T. Ertl. Efficiently Using Graphics Hardware in Volume Rendering Applications. *Computer Graphics (SIGGRAPH '98)*, 32(4):169–179, 1998.